Eur Radiol (2014) 24:3134–3141
DOI 10.1007/s00330-014-3355-y

HEPATOBILIARY-PANCREAS

Does secretin stimulation add to magnetic resonance cholangiopancreatography in characterising pancreatic cystic lesions as side-branch intraductal papillary mucinous neoplasm?

Andrei S. Purysko · Namita S. Gandhi · R. Mathew Walsh · Nancy A. Obuchowski · Joseph C. Veniero

Received: 25 December 2013 / Revised: 13 July 2014 / Accepted: 16 July 2014 / Published online: 7 August 2014

Abstract
Objectives To assess the value of secretin during magnetic resonance cholangiopancreatography (MRCP) in demonstrating communication between cystic lesions and the pancreatic duct to help determine the diagnosis of side-branch intraductal papillary mucinous neoplasm (SB-IPMN).
Methods This is an IRB-approved, HIPAA-compliant retrospective study of 29 SB-IPMN patients and 13 non-IPMN subjects (control) who underwent secretin-enhanced MRCP (s-MRCP). Two readers blinded to the final diagnosis reviewed three randomised image sets: (1) pre-secretin HASTE, (2) dynamic s-MRCP and (3) post-secretin HASTE. Logistic regression, generalised linear models and ROC analyses were used to compare pre- and post-secretin results.
Results There was no significant difference in median scores for the pre-secretin [reader 1: 1; reader 2: 2 (range -2 to 2)] and post-secretin HASTE [reader 1: 1; reader 2: 1 (range -2 to 2)] in the SB-IPMN group (P=0.14), while the scores were lower for s-MRCP [reader 1: 0.5 (range -2 to 2); reader 2: 0 (range -1 to 2); P=0.016]. There was no significant difference in mean maximum diameter of SB-IPMN on pre- and post-secretin HASTE, and s-MRCP (P>0.05).
Conclusion Secretin stimulation did not add to MRCP in characterising pancreatic cystic lesions as SB-IPMN.

A. S. Purysko (✉) · N. S. Gandhi · J. C. Veniero
From the Abdominal Imaging Section, Imaging Institute, Cleveland Clinic, 9500 Euclid Ave, Cleveland, OH 44195, USA
e-mail: puryska@ccf.org

R. M. Walsh
Department of General Surgery, Digestive Disease Institute, Cleveland Clinic, 9500 Euclid Ave, Cleveland, OH 44195, USA

N. A. Obuchowski
Department of Quantitative Health Sciences, Cleveland Clinic, 9500 Euclid Ave, Cleveland, OH 44195, USA

Key Points
- *Magnetic resonance cholangiopancreatography (MRCP) is used to evaluate pancreatic cystic lesions.*
- *Intraductal papillary mucinous neoplasm (IPMN) is a type of pancreatic cystic neoplasm.*
- *Secretin administration does not facilitate the diagnosis of IPMN on MRCP.*

Keywords Magnetic resonance imaging · Secretin · Pancreatic neoplasms · Intraductal papillary mucinous neoplasm · Pancreatic cyst

Abbreviations

MRCP	magnetic resonance cholangiopancreatography
S-MRCP	secretin-enhanced magnetic cholangiopancreatography
IPMN	intraductal papillary mucinous neoplasm, SB-IPMN, side-branch intraductal papillary mucinous neoplasm
MDCT	multidetector computed tomography
HASTE	half-Fourier acquisition single-shot turbo spin-echo
MPD	main pancreatic duct

Introduction

Intraductal papillary mucinous neoplasm (IPMN) is a type of pancreatic cystic tumour described recently in other studies [1, 2]. Histologically, these tumours are characterised by intraductal proliferation of neoplastic mucin-producing cells associated with papillary projections [2, 3]. The tumours are classified according to whether there is involvement of the main pancreatic duct (MPD-IPMN), isolated side branches

(SB-IPMN), or both (mixed IPMN). IPMNs have malignant potential, which is significantly greater in tumours involving the MPD. According to pooled data from multiple published series of ≥50 cases, the mean frequency of malignancy in MD-IPMN is 61.6 % (range, 36-100 %), and the mean frequency of invasive cancer is 43.1 % (range, 11-81 %), while the mean frequency of malignancy in BD-IPMN is 25.5 % (range, 6.3-46.5 %) and the mean frequency of invasive cancer is 17.7 % (range, 1.4-36.7 %) [4]. Because of the high malignant potential, surgical resection is in general recommended for MPD-IPMN. Conversely, SB-IPMNs are managed more conservatively with imaging surveillance, especially in asymptomatic patients with cysts measuring <3 cm and without features considered worrisome for malignancy (e.g. mural nodules; thick, enhancing walls) [4, 5].

The increase in IPMN diagnoses in recent decades has been attributed to the widespread use of cross-sectional imaging with multidetector computed tomography (MDCT) and magnetic resonance (MR) imaging [6]. Many incidental lesions are ≤1 cm, which makes accurate diagnosis more challenging [5]. Excessive mucin production by the neoplastic cells results in dilation of the pancreatic ductal system, which is one of the major characteristic findings of these tumours [7]. SB-IPMN may demonstrate a more segmental cystic appearance that can mimic the appearance of other cystic neoplasms of the pancreas, such as mucinous cystic neoplasms and non-neoplastic cysts. Visualisation of the communication between the SB-IPMN and the pancreatic duct system is a key feature that allows us to distinguish IPMNs from cystic lesions of other aetiologies [4, 5, 8].

Magnetic resonance cholangiopancreatography (MRCP) uses the almost stationary fluid in the biliary and pancreatic ductal system as an intrinsic contrast medium and allows detailed evaluation of the biliary and pancreatic ductal anatomy [7, 9]. Both the 2012 International Consensus Guidelines for the Management of IPMN and MCN of the pancreas [4] and the American College of Radiology (ACR) white paper on incidental findings on abdominal computed tomography [5] recommend this non-invasive test as the imaging modality for the initial evaluation and follow-up of pancreatic cystic lesions, and in cases of IPMN, this modality can be used to asses features predictive of malignancy [10, 11].

One recent refinement of the MRCP is the potential addition of synthetic human secretin during the examination [10, 12]. The hormone secretin is produced by secretin cells (or "S cells") in the duodenum, and it stimulates the pancreatic exocrine function in response to a decrease in pH caused by the passage of gastric contents [13]. Intravenous administration of secretin during MRCP also stimulates pancreatic exocrine function resulting in increased excretion of pancreatic fluid into the pancreatic ducts, changing their signal and calibre [14]. It has been suggested that secretin-enhanced MRCP (s-MRCP) could therefore facilitate the diagnosis of IPMN either directly by allowing or improving the visibility of a communication between the MPD and the cystic lesion or indirectly by showing increased cyst size or signal intensity [10–12]. Some authors have suggested that s-MRCP should be performed in the initial evaluation of pancreatic cystic lesions to demonstrate the relationship between the lesions and the MPD [12, 15].

The purpose of our study was to assess the value of adding secretin stimulation to MRCP to aid in the diagnosis of SB-IPMN by demonstrating communication between cystic pancreatic lesions and the MPD, or a change in lesion size.

Materials and methods

Patient selection

Institutional review board approval was obtained and informed consent was waived for this retrospective, Health Insurance Portability and Accountability Act-compliant study.

A search of our institution's radiology report database identified 215 consecutive patients who underwent s-MRCP between January 2007 and October 2009 (Fig. 1). Patients were initially considered candidates for the study if the s-MRCP was being performed to investigate one or more pancreatic cystic lesions measuring ≥1 cm (n=45). Patients were subsequently excluded from the study for the following reasons: incomplete sets of images available for review in the picture archiving and communication system (n=5), presence of innumerable cystic lesions precluding adequate visualisation of the MPD (n=2), inappropriate selection of the plane of imaging acquisition (n=1) and no detectable cystic lesion on MRCP images (n=1).

Of the 36 patients included in our study, SB-IPMN was diagnosed in 23 patients [12 men, 11 women; mean age, 63.2 years (range, 45-82.5 years)]. In these 23 patients, the final diagnosis of SB-IPMN was based on histopathology from surgical specimen in 6 patients; findings on endoscopic ultrasound and fine-needle aspiration with cyst fluid analysis and cytology in 19 patients; and imaging appearance (definite communication with main pancreatic duct demonstrated by both MRCP and EUS examinations) in 1 patient.

The control group was composed of the remaining 13 patients [8 men, 5 women; mean age, 55.8 years (range, 37-71.5 years)] who presented with an alternative diagnosis, including pancreatic pseudocysts (n=8), mucinous cystadenomas (n=3) and serous cystadenomas (n=2). The diagnostic workup in these 13 patients included endoscopic ultrasound with fine-needle aspiration in eight patients, surgical resection in four patients and imaging diagnosis in one patient (pancreatic serous cystadenoma with characteristic imaging appearance). All patients included in the study were clinically assessed by a multidisciplinary team of physicians

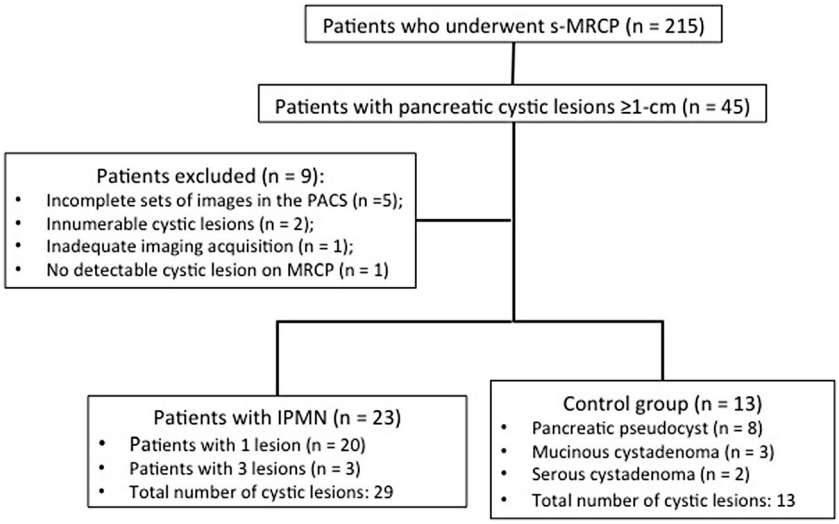

Fig. 1 Flow diagram of patient selection and inclusion and exclusion criteria for the study. *s-MRCP* secretin-enhanced magnetic cholangiopancreatography, *PACS* picture archiving and communication system, *IPMN* intraductal papillary mucinous neoplasm

with extensive experience in the care of patients with pancreatic neoplasm.

Imaging technique

Approximately 30 min prior to the examination, 300 ml of silicone-coated,

superparamagnetic iron oxide oral MR contrast agent [ferumoxsil oral suspension (Gastromark), Mallinckrodt Medical, Raleigh, NC] was administered. This agent has T2-shortening properties and helps to avoid obscuration of the high signal intensity fluid in the pancreatic ducts by high signal intensity fluid in the overlying stomach and duodenum.

The s-MRCP examinations were performed on 1.5-T MR systems (Avanto, Espree, or Symphony; Siemens Healthcare, Erlangen, Germany) using a torso phased-array coil. After scout images had been obtained, axial and coronal half-Fourier acquisition single-shot turbo spin-echo (HASTE) images [slice thickness, 4 mm; repetition time (TR)/echo time (TE), 500-727/63-72 ms; flip angle, 160-180°; echo-train length, 256; matrix, 256×256 coronal and 256×176 axial] were obtained through the abdomen. An intravenous test dose of 0.2 μg of secretin (ChiRhoStim; ChiRhoClin, Inc., Burtonsville, MD) was administered before the study. If the patient did not develop any secondary effects to the secretin test dose, the s-MRCP was performed, during which an additional 0.2 μg/kg of secretin was administered over a period of 1 min at the appropriate time during the study. At that time, dynamic "thick-slab" s-MRCP sequences (slice thickness, 60 mm; TR/TE, 3,000/972 ms; flip angle, 150°; matrix, 256×256) were obtained every 30 s for 10 min. Finally, after the 10-min dynamic assessment, another set of axial and coronal HASTE images was obtained through the abdomen with the same parameters as used before secretin administration (Fig. 2).

Imaging interpretation

Three sets of anonymised images were created for each patient. The first set contained the HASTE images obtained in both the axial and coronal planes before secretin stimulation; the second set contained all 20 images from the dynamic s-MRCP sequence; and the third set contained the HASTE images obtained in both axial and coronal planes after secretin stimulation. These three sets were anonymised and randomised and independently reviewed on a workstation (Leonardo; Siemens Healthcare) by two radiologists with subspecialties in abdominal imaging and with more than 10 and 5 years of experience in the field; both radiologists were blinded to the final diagnosis of each patient.

The readers were not aware of whether the HASTE image sets were pre- or post-secretin stimulation. Each reader was asked to assign a confidence score for the communication between each individual cystic lesion measuring ≥1 cm and the MPD, on all three entire image sets, based on the following five-point scale: +2, definitely communicates; +1, probably communicates; 0, indeterminate; –1, probably does not communicate; –2; definitely does not communicate. The readers were also asked to measure the diameter of each individual cystic lesion on the image sets.

Statistical analysis

Differences in the assigned confidence score for ductal communication were categorised as follows: increase in confidence score from pre-secretin phase, +1; no change in the score from pre-secretin phase, 0; decrease in the score from pre-secretin phase, –1. A logistic regression model was fit to test whether there was a change in confidence score from the pre-secretin phase to the post-secretin phase. The dependent variable in the model was a binary variable denoting an increase or decrease in confidence score after secretin

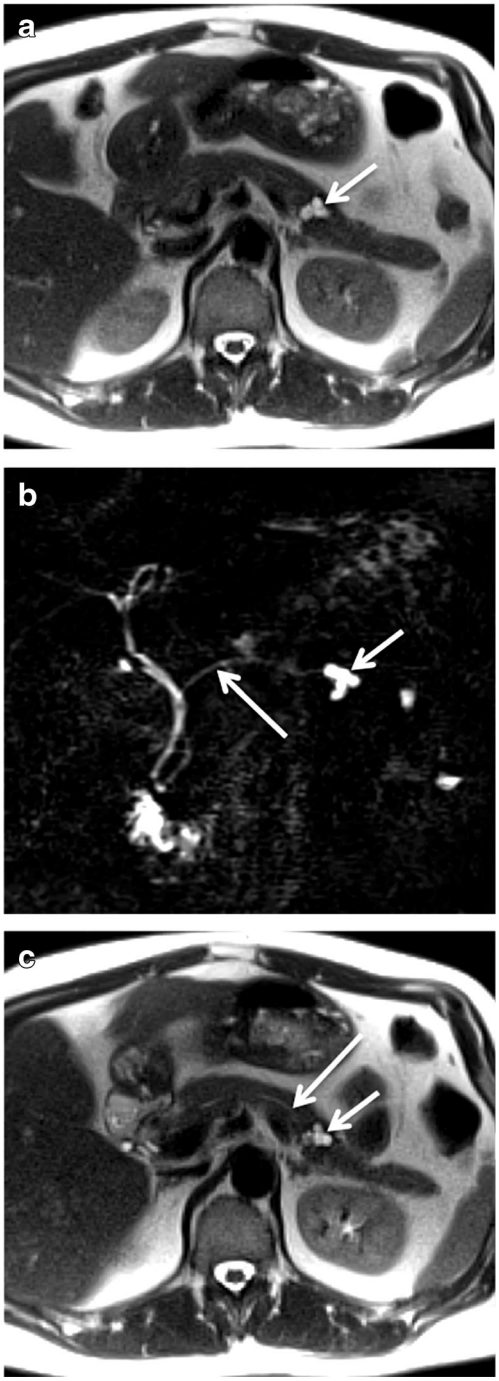

Fig. 2 S-MRCP images of a patient with an IPMN. (**a**) Axial HASTE image pre-secretin, (**b**) dynamic s-MRCP image and (**c**) axial HASTE image post-secretin. A pancreatic cystic lesion (*short thin arrow* on **a**, **b** and **c**) is noted at the junction of the pancreatic body and tail. The main pancreatic duct is better seen on the dynamic s-MRCP image (*long thin arrow* on **b**). A small increase (1-2 mm) in the calibre of the main pancreatic duct is noted on HASTE images after secretin stimulation (*long thin arrow* on **c**) compared to pre-secretin HASTE images, but did not significantly improve the ability to determine the communication between the cystic pancreatic lesion and the main pancreatic duct. Sagittal and coronal HASTE images pre- and post-secretin stimulation (not shown) are also obtained as part of the protocol. *HASTE* half-Fourier acquisition single-shot turbo spin echo

stimulation (cases of no change were omitted from this analysis). The independent variable in the model was the reader. Separate models were built for the two groups. Generalised estimating equation GEEs were used with an exchangeable correlation structure to account for multiple observations on the same patient. A significance level of 0.05 was applied.

To assess the diagnostic accuracy of readers in distinguishing IPMN from non-IPMN lesions, nonparametric estimates of the area under the receiver-operating characteristic (ROC) curve were calculated for each reader pre- and post-secretin. The null hypothesis that the ROC area equals 0.5 (chance) was evaluated using a Wald test; a significance level of 0.05 was applied.

Generalised linear models were fit to test whether the cystic lesion size changed between the pre-secretin HASTE and post-secretin stimulation phases (HASTE and dynamic s-MRCP). The dependent variable in the model was the cystic lesion post-secretin size minus the pre-secretin size. The independent variable in the model was the reader. GEEs were used with an exchangeable correlation structure to account for multiple observations on the same patient. Separate models were built for the IPMN group and the control group. A Wald test was used to evaluate whether the intercept differed from zero. A significance level of 0.05 was applied.

Results

Confidence scores for the communication between the pancreatic cystic lesions and the MPD

There was no statistically significant difference in median confidence scores assigned on the HASTE images pre- and post-secretin stimulation for the IPMN group (P=0.14) or the control group (P=0.53) (Table 1). For reader 1, in the IPMN group, the confidence scores for the HASTE images before secretin stimulation were higher in 10 cystic lesions, equal in 15 and lower in 4 compared to HASTE images after secretin stimulation; for reader 2, the confidence scores for the HASTE images before secretin stimulation were higher in 7 cystic lesions, equal in 19 and lower in 3 compared HASTE images after secretin stimulation. For reader 1, in the control group, the confidence scores for the HASTE images before secretin stimulation were higher in four cystic lesions, equal in seven and lower in two compared to HASTE images after secretin stimulation; for reader 2, the confidence scores for the HASTE images before secretin stimulation were higher in four cystic lesions, equal in three and lower in six compared to HASTE images after secretin stimulation.

With the dynamic s-MRCP sequence, the readers were not able to identify two SB-IPMN lesions that were seen on the HASTE images before secretin stimulation. For the remainder

Table 1 Comparison between the assigned ductal communication score between the HASTE images pre- and post-secretin stimulation

IPMNs (n=29)	Reader 1		Reader 2		P value
	Pre-secretin	Post-secretin	Pre-secretin	Post-secretin	
Median score (range)	1.0 (-2 to 2)	1.0 (-2 to 2)	2.0 (-2 to 2)	2.0 (-2 to 2)	0.14
HASTE pre-secretin>post-secretin (n=10)			HASTE pre-secretin>post-secretin (n=7)		
HASTE pre-secretin=post-secretin (n=15)			HASTE pre-secretin=post-secretin (n=19)		
HASTE pre-secretin<post-secretin (n=4)			HASTE pre-secretin<post-secretin (n=3)		
Control group (n=13)	Reader 1		Reader 2		P value
	Pre-secretin	Post-secretin	Pre-secretin	Post-secretin	
Median score (range)	1.0 (-2 to 2)	1.0 (-2 to 2)	1.0 (-2 to 2)	1.0 (-2 to 2)	0.53
HASTE pre-secretin>post-secretin (n=4)			HASTE pre-secretin>post-secretin (n=4)		
HASTE pre-secretin=post-secretin (n=7)			HASTE pre-secretin=post-secretin (n=3)		
HASTE pre-secretin<post-secretin (n=2)			HASTE pre-secretin<post-secretin (n=6)		

of the cystic lesions that could be identified on both image sets, the median confidence score on the pre-secretin HASTE images for the SB-IPMN group was significantly higher than the median score on the dynamic s-MRCP (P=0.016). For reader 1, in the IPMN group, the confidence scores for the HASTE images before secretin stimulation compared to dynamic s-MRCP images were higher in 12 cystic lesions, equal in 7 and lower in 8; for reader 2, the confidence scores for the HASTE images before secretin stimulation compared HASTE images after secretin stimulation were higher in 15 cystic lesions, equal in 8 and lower in 4.

In the control group, no statistically significant difference in the median scores was identified for either reader (P= 0.413) (Table 2). For reader 1, in the control group, the confidence scores for the HASTE images before secretin stimulation were higher in ten cystic lesions, equal in one and lower in two compared to dynamic s-MRCP images; for reader 2, the confidence scores for the HASTE images before secretin stimulation were higher in seven cystic lesions, equal in two and lower in four compared to dynamic s-MRCP images.

The readers' ROC areas for distinguishing the IPMN and non-IPMN lesions pre-secretin were 0.61 and 0.69, respectively. The readers' ROC areas post-secretin were similar, 0.56 and 0.57, respectively, which did not differ significantly from chance.

Changes in maximum diameter of the cystic lesions

There was no statistically significant difference in the mean maximum diameters measured by readers on the pre- and post-secretin HASTE images for the SB-IPMN group (P= 0.99) and the control group (P=0.68) (Table 3). The readers' estimated ROC areas pre-secretin were 0.72 and 0.68, and post-secretin were 0.71 and 0.69, respectively. The ROC areas were significantly different from 0.5 (chance value) but there was no improvement in ROC area with secretin. For the cystic lesions that could be identified on both pre-secretin HASTE and dynamic s-MRCP, there was no significant difference in the mean maximum diameters for the SB-IPMN group. However, the mean maximum diameter of the cystic lesions in the

Table 2 Comparison between the assigned ductal communication score between the HASTE pre-secretin stimulation and the dynamic s-MRCP images

IPMNs (n=27)	Reader 1		Reader 2		P value
	Pre-secretin	Dynamic	Pre-secretin	Dynamic s-MRCP	
Median score (range)	1.0 (-2 to 2)	0.5 (-2 to 2)	2.0 (-2 to 2)	2.0 (-1 to 2)	0.016
HASTE pre-secretin>dynamic s-MRCP (n=12)			HASTE pre-secretin>dynamic s-MRCP (n=15)		
HASTE pre-secretin=dynamic s-MRCP (n=7)			HASTE pre-secretin=dynamic s-MRCP (n=8)		
HASTE pre-secretin<dynamic s-MRCP (n=8)			HASTE pre-secretin<dynamic s-MRCP (n=4)		
Control group (n=13)	Reader 1		Reader 2		P value
	Pre-secretin	Dynamic	Pre-secretin	Dynamic s-MRCP	
Median score (range)	1.0 (-2 to 2)	1.0 (-2 to 2)	1.0 (-2 to 2)	1.0 (-2 to 2)	0.53
HASTE pre-secretin>dynamic s-MRCP (n=10)			HASTE pre-secretin>dynamic s-MRCP (n=7)		
HASTE pre-secretin=dynamic s-MRCP (n=1)			HASTE pre-secretin=dynamic s-MRCP (n=2)		
HASTE pre-secretin<dynamic s-MRCP (n=2)			HASTE pre-secretin<dynamic s-MRCP (n=4)		

Table 3 Maximum diameter (cm) of the cystic pancreatic lesions

HASTE pre-secretin vs. HASTE post-secretin		Reader 1		Reader 2		*P* value
		Pre-secretin	Post-secretin	Pre-secretin	Post-secretin	
IPMN (*n*=29)	Mean (SD)	2.4 (1.1)	2.4 (1.2)	2.3 (1)	2.2 (0.9)	0.99
Control (*n*=13)	Mean (SD)	2.9 (1.0)	2.9 (1.0)	2.8 (1.1)	2.7 (1.1)	0.68
HASTE pre-secretin vs. dynamic s-MRCP		Reader 1		Reader 2		*P value*
		Pre-secretin	Dynamic s-MRCP	Pre-secretin	Dynamic s-MRCP	
IPMN (*n*=27)	Mean (SD)	2.4 (1.2)	2.4 (1.2)	2.2 (1.0)	2.1 (1.1)	0.69
Control (*n*=13)	Mean (SD)	2.9 (1.1)	2.8 (1.0)	2.9 (1.1)	2.4 (1.1)	0.044

control group was smaller on the dynamic s-MRCP than on the pre-secretin HASTE images (P=0.044).

Discussion

Secretin administration did not improve the demonstration of direct or indirect signs of communication between the SB-IPMN and the MPD. There was no significant difference in the readers' confidence for communication between the cystic lesion and the MPD on the pre- and post-secretin HASTE sequences, though the readers' confidence was significantly lower in the dynamic phase for the SB-IPMN group. There was no significant difference in the size of the cystic lesion before and after secretin administration.

Morphologic changes in the pancreatic ducts secondary to secretin stimulation during MRCP were initially reported by Matos et al. [16]. In this study, which included healthy volunteers and patients with suspected pancreatitis, the MPD was visualised in all patients (*n*=23) after secretin stimulation. However, only a single SB was demonstrated after secretin stimulation in a patient with suspected pancreatitis, and no SBs were demonstrated in healthy participants. In a study conducted by Hellerhof et al. [17] that included a larger number of patients (*n*=95), the visualisation of SBs was significantly improved with secretin stimulation only in the group of patients with chronic pancreatitis (21 of 23 patients). The findings of these two studies suggest that, with the exception of patients with chronic pancreatitis, who may have some degree of baseline dilation of the SBs, the effect of secretin stimulation may not be sufficient to produce changes in the SBs that can be depicted by MRCP imaging. These findings were echoed in a study by Fukukura et al. [18], in which secretin stimulation improved the visualisation of SBs in just 14 of 85 (16 %) healthy patients.

These previous results help to explain the findings in our study, in which secretin stimulation did not improve the demonstration of a communication between SB-IPMNs and the MPD (Fig. 3). Even if dilation of a SB was detected after secretin stimulation, this could potentially negatively affect a clinician's ability to determine whether a communication is present. For instance, if a cystic lesion other than an IPMN is too close to a dilated SB, it may be difficult to determine with

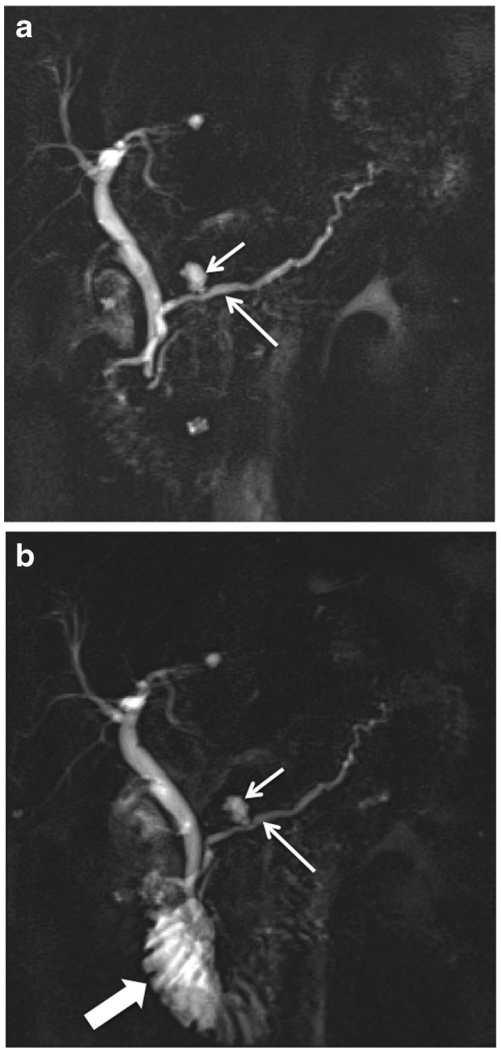

Fig. 3 Dynamic thick-slab s-MRCP images. (**a**) Baseline image and (**b**) 5-min post-secretin administration image at peak effect of secretin. A side-branch IPMN in the pancreatic body (*short thin arrow* on **a** and **b**) appears to communicate with the main pancreatic duct (*long thin arrow* on **a** and **b**) on the baseline image, with no significant change after secretin administration. Notice the lack of significant changes in pancreatic duct side branches after secretin stimulation. A normal amount of pancreatic fluid is excreted into the duodenum after secretin stimulation (*thick arrow* on **b**)

certainty the absence of a communication. In fact, reader 1 assigned higher confidence scores for ductal communication after secretin stimulation on HASTE and dynamic s-MRCP sequences in two cystic lesions of the control group, while reader 2 assigned higher scores in six cystic lesions of the control group on the post-secretin HASTE and higher scores in four cystic lesions of the control group on the dynamic s-MRCP sequence.

Carbognin et al. [12] found that secretin administration was useful in increasing MRCP sensitivity in the detection of the communicating duct of branch duct IPMTs although the details of the study are not available. Interestingly, in their abstract, the most common site of collateral branch IPMTs was the body/tail, while the most common site of side branch IPMT is known to be the head and uncinate process. Also, (1) the number of readers, (2) whether they were blinded and (3) how the data were recorded are not clear from the abstract.

The cystic portion of an IPMN is lined by columnar mucinous epithelium that has morphologic characteristics similar to those of gastric foveolar epithelium [19]. While secretin stimulates the normal duct cells of the pancreas to secrete fluid and bicarbonate, it is not clear whether secretin also has secretory effects in the mucin-producing neoplastic epithelium of ducts involved in IPMNs [13]. Additionally, the presence of mucin and cellular material in a distinct SB duct may hinder the ability of the SB to dilate during secretin stimulation. These factors may account for the lack of statistically significant change in the maximum diameter and signal intensity of SB-IPMNs after secretin stimulation in our study.

A few specific technical aspects of the s-MRCP protocol may also affect its performance for this particular application. The dynamic thick-slab s-MRCP phase is obtained in a single oblique plane oriented along the plane of the main pancreas and duodenum with a large field of view. While this allows for detection of the pancreatic fluid excreted in response to secretin stimulation, it is suboptimal for visualisation of entire pancreatic cystic lesion and its relationship with the pancreatic duct. These deficiencies may have contributed to the lower scores assigned to the SB-IPMN group on the dynamic phase as compared to the pre-secretin HASTE images and to the lower mean maximum diameter of the lesions in the control group measured in this sequence (Table 3).

The maximum dilation of the pancreatic ducts occurs approximately 4 to 5 min after secretin administration [18]. The post-secretin HASTE images are obtained after the acquisition of the dynamic s-MRCP sequence, which takes 10 min. Therefore, the time of acquisition of the post-secretin HASTE images is beyond the time of maximal effect of secretin on the pancreatic ductal system and most of the secreted fluid has already passed in the duodenum. This potentially affects the visualisation of duct communication on the post-secretin HASTE images and explains the lack of significant difference in duct communication and the lesion size on the pre- and post-secretin HASTE images (Table 1).

Our study had several limitations, including its retrospective nature and the relatively small number of patients. Other imaging features that could have influenced the diagnosis of SB-IPMN (e.g., multiplicity) were not evaluated, which may have introduced some bias in reader assessments. Additionally, most but not all cystic lesions had histological confirmation (one cystic lesion from each group).

In conclusion, secretin enhancement did not add to the diagnostic value of MRCP in characterising pancreatic cystic lesions as SB-IPMN or non-IPMN, with no significant difference observed in the demonstration of communication between cystic pancreatic lesions and the MPD. The results of this study do not support the routine use of secretin during MRCP to improve the characterisation of cystic pancreatic lesions as SB-IPMN.

Acknowledgments The scientific guarantor of this publication is Namita S. Gandhi, MD. The authors of this manuscript declare no relationships with any companies, whose products or services may be related to the subject matter of the article. The authors state that this work has not received any funding. One of the authors has significant statistical expertise. Institutional Review Board approval was obtained. Written informed consent was waived by the Institutional Review Board. Methodology: retrospective, diagnostic, performed at one institution

References

1. Rickaert F, Cremer M, Devière J et al (1991) Intraductal mucin-hypersecreting neoplasms of the pancreas. A clinicopathologic study of eight patients. Gastroenterology 101:512–519
2. Kloppel G, Solcia E, Longnecker DS, Capella C, Sobin LH (1996) Histological typing of tumours of the exocrine pancreas. In: World Health Organization International Histological Classification of Tumors, 2nd edn. Springer, Berlin, pp 11–20
3. Adsay NV (2007) Cystic lesions of the pancreas. Mod Pathol 20: S71–S93
4. Tanaka M, Fernández-del Castillo C, Adsay V et al (2012) International Association of Pancreatology. International consensus guidelines 2012 for the management of IPMN and MCN of the pancreas. Pancreatology 12:183–197
5. Berland LL, Silverman SG, Gore RM et al (2010) Managing incidental findings on abdominal CT: white paper of the ACR incidental findings committee. J Am Coll Radiol 7:754–773
6. Guarise A, Faccioli N, Ferrari M et al (2008) Evaluation of serial changes of pancreatic branch duct intraductal papillary mucinous neoplasms by follow-up with magnetic resonance imaging. Cancer Imaging 8:220–228
7. Lim JH, Lee G, Oh YL (2001) Radiologic spectrum of intraductal papillary mucinous tumor of the pancreas. Radiographics 21:323–337
8. Pedrosa I, Boparai D (2010) Imaging considerations in intraductal papillary mucinous neoplasms of the pancreas. World J Gastrointest Surg 2:324–330
9. Kalb B, Sarmiento JM, Kooby DA, Adsay NV, Martin DR (2009) MR imaging of cystic lesions of the pancreas. Radiographics 29: 1749–1765

10. Waters JA, Schmidt CM, Pinchot JW et al (2008) CT vs MRCP: optimal classification of IPMN type and extent. J Gastrointest Surg 12:101–109
11. Manfredi R, Graziani R, Motton M et al (2009) Main pancreatic duct intraductal papillary mucinous neoplasms: accuracy of MR imaging in differentiation between benign and malignant tumors compared with histopathologic analysis. Radiology 253:106–115
12. Carbognin G, Pinali L, Girardi V, Casarin A, Mansueto G, Mucelli RP (2007) Collateral branches IPMTs: secretin-enhanced MRCP. Abdom Imaging 32:374–380
13. Chey WY, Chang TM (2003) Secretin, 100 years later. J Gastroenterol 38:1025–1035
14. Sanyal R, Stevens T, Novak E, Veniero JC (2012) Secretin-enhanced MRCP: review of technique and application with proposal for quantification of exocrine function. AJR Am J Roentgenol 198:124–132
15. Tirkes T, Sandrasegaran K, Sanyal R et al (2013) Secretin-enhanced MR cholangiopancreatography: spectrum of findings. Radiographics 33:1889–1906
16. Matos C, Metens T, Deviere J et al (1997) Pancreatic duct: morphologic and functional evaluation with dynamic MR pancreatography after secretin stimulation. Radiology 203:435–441
17. Hellerhoff KJ, Helmberger H 3rd, Rösch T, Settles MR, Link TM, Rummeny EJ (2002) Dynamic MR pancreatography after secretin administration: image quality and diagnostic accuracy. AJR Am J Roentgenol 179:121–129
18. Fukukura Y, Fujiyoshi F, Sasaki M, Nakajo M (2002) Pancreatic duct: morphologic evaluation with MR cholangiopancreatography after secretin stimulation. Radiology 222:674–680
19. Fernádez-del Castillo C, Adsay NV (2010) Intraductal papillary mucinous neoplasm of the pancreas. Gastroenterology 139:708–713